Published in final edited form as:
Chem Res Toxicol. 2011 June 20; 24(6): 797–808. doi:10.1021/tx100447k.

REACTION OF CRESYL SALIGENIN PHOSPHATE, THE ORGANOPHOSPHORUS AGENT IMPLICATED IN THE AEROTOXIC SYNDROME, WITH HUMAN CHOLINESTERASES: MECHANISTIC STUDIES EMPLOYING KINETICS, MASS SPECTROMETRY AND X-RAY STRUCTURE ANALYSIS

Eugénie Carletti[1], **Lawrence M. Schopfer**[2], **Jacques-Philippe Colletier**[1], **Marie-Thérése Froment**[3], **Florian Nachon**[3], **Martin Weik**[1], **Oksana Lockridge**[2], and **Patrick Masson**[1,2,3,*]

[1] Laboratoire de Biophysique Moléculaire, Institut de Biologie Structurale, 41 rue Jules Horowitz, 38027 Grenoble, France

[2] Eppley Institute and Department of Biochemistry and Molecular Biology, University of Nebraska Medical Center, Omaha, Nebraska 68198-5950, USA

[3] Département de Toxicologie, Institut de Recherche Biomédicale des Armées (IRBA)-Centre de Recherches du Service de Santé des Armées (CRSSA), 24 av des Marquis du Grésivaudan, 38702 La Tronche, France

Abstract

The aerotoxic syndrome is assumed to be caused by exposure to tricresyl phosphate (TCP), an anti-wear additive in jet engine lubricants and hydraulic fluids. CBDP (2-(ortho-cresyl)-4H-1,2,3-benzodioxaphosphoran-2-one) is the toxic metabolite of tri-ortho-cresylphosphate, a component of TCP. Human butyrylcholinesterase (BChE; EC 3.1.1.8) and human acetylcholinesterase (AChE; EC 3.1.1.7) are irreversibly inhibited by CBDP. The bimolecular rate constants of inhibition (k_i), determined under pseudo first-order conditions, displayed a biphasic time course of inhibition with k_i 1.6×10^8 $M^{-1}min^{-1}$ and 2.7×10^7 $M^{-1}min^{-1}$ for E and E′ forms of BChE. The inhibition constants for AChE were one to two orders of magnitude slower than for BChE. CBDP-phosphorylated cholinesterases are non-reactivatable due to ultra fast “aging”. Mass spectrometry analysis showed an initial BChE adduct with an added mass of 170 Da from cresylphosphate, followed by dealkylation to a structure with an added mass of 80 Da. Mass spectrometry in ^{18}O–water showed that ^{18}O was incorporated only during the final aging step to form phospho-serine as the final “aged” BChE adduct. The crystal structure of CBDP-inhibited BChE confirmed that the phosphate adduct is the ultimate aging product. CBDP is the first organophosphorus agent that leads to a fully dealkylated phospho-serine BChE adduct.

Keywords

Acetylcholinesterase; butyrylcholinesterase; aerotoxic syndrome; organophosphate; CBDP; inhibition kinetics; aging; MALDI-TOF; X-ray crystallography; OPIDN; saligenin

Correspondence: Prof. Patrick Masson, pmasson@unmc.edu.

Introduction

The cyclic organophosphorus agent 2-(o-cresyl)-4H-1,3,2-benzodioxaphosphoran-2-one (CBDP), also called cresyl saligenin phosphate, has been implicated in development of organophosphate-induced delayed neuropathy (OPIDN) (1). OPIDN is a paralytic condition that is distinct from the toxicity associated with organophosphate inhibition of acetylcholinesterase (AChE) (2). Well known incidents of OPIDN have been attributed to the consumption of Jamaica ginger, a folk medicine, adulterated with tri-o-cresyl phosphate (TOCP) (3), and to the consumption of cooking oil adulterated with jet engine oil containing TOCP (4). The toxicity of TOCP has been attributed to its conversion into CBDP, *in vivo* (5,6). CBDP is formed *in vivo* by two consecutive reactions: 1) liver microsomal cytochrome P450-catalyzed oxidation (6), and 2) serum albumin-catalyzed cyclization of the oxidation product (7) (Scheme 1).

TOCP is a component of tri-cresyl phosphate (TCP) that is a combination of ten tri-cresyl phosphate isomers (tri-ortho, tri-para, tri-meta, and mixtures of the three). TOCP is more toxic than the para and meta isomers (8). TCP is used as an anti-wear/extreme pressure agent and flame retardant in jet hydraulic fluids and engine oils (8,9). Due to its toxicity, the level of TOCP in commercial TCP mixtures has been reduced over time (8). However, it is unclear whether this precaution has been sufficient to prevent toxic exposure to TOCP because safe levels of exposure are still in dispute (10).

Over the past 30 years, an increasing number of reports have appeared documenting the occurrence of neurological signs associated with air travel, both commercial and military (10). Short-term symptoms include blurred vision, dizziness, confusion, headache, tremors, nausea, vertigo, shortness of breath, increased heart rate, and irritation of the eyes and nose. Long-term symptoms include memory loss, numbness, lack of co-ordination, sleep disorders, severe headaches, nausea, diarrhea, susceptibility to upper respiratory infection, chest pain, skin blisters, signs of immunosuppression, muscle weakness, muscle pain, and fatigue (10,11). The term aerotoxic syndrome has recently been coined to describe this condition (10). Fumes escaping from the engine through leaky oil seals into the bleed air of the aircraft cabin are suspected to be the source of the toxicants that cause aerotoxic syndrome (8,10).

Toxic components of these fumes include hexane, CO, CO_2 and TOCP. TOCP after bio-activation to CBDP is suspected of being responsible for the symptoms. A key gap in the evidence trail between fumes and syndrome is a quantitative biomarker for exposure to TOCP. CBDP has long been known as an inhibitor of carboxylesterases (12,13,14) and of neuropathy target esterase (15). Animal studies have shown that CBDP is also an irreversible inhibitor of both AChE and BChE (12,16). However, *in vitro* studies have indicated that CBDP reacts slowly with mammalian ChEs (14,17). Modifications to the structure of CBDP have led to the development of insecticides, such as salioxon (2-methoxy-4H-1,3,2-benzodioxaphosphorin 2-oxide), that display strong anti-cholinesterase activity (18,19,20). Recently, we established that human BChE reacts with CBDP. The organophosphorylated adduct undergoes two consecutive dealkylation reactions, i.e. aging, forming an ultimate phosphate adduct on the active site serine (Ser198) (1). This phosphorylated derivative is unique in the study of organophosphate (OP) reactions with BChE, and therefore would be an ideal candidate for use as a biomarker of exposure to TOCP. Interest in BChE as a biomarker for exposure to TOCP has prompted us to investigate the mechanism and kinetics of the reaction of CBDP with BChE and AChE in more detail.

In the present report, we 1) investigated the kinetics of phosphorylation, inhibition and aging of highly purified human AChE and human BChE by CBDP; 2) examined the chemistry for formation of the post-phosphorylation adducts, using mass spectrometry and ^{18}O-water; and 3) determined the X-ray structure of the ultimate aged conjugate of CBDP-phosphoryated human BChE.

The kinetics for the reaction of CBDP with human BChE indicate that CBDP is one of the most potent OP inhibitors for BChE heretofore discovered, and that post-phosphorylation aging is extremely rapid. Because of this high reactivity, BChE very likely plays a role in protection against toxicity of TOCP by scavenging CBDP from the human blood stream. Both X-ray crystallography and mass spectrometry confirm that the ultimate product from the reaction of CBDP with BChE is a novel phosphorylated adduct of the catalytic serine, Ser198.

Kinetics for the reaction of CBDP with human AChE indicate that AChE is significantly sensitive to CBDP, although less than BChE by at least one order of magnitude.

Materials and Methods

Caution

CBDP is a highly toxic organophosphorus compound. Handling requires suitable personal protection, training, and facilities. These requirements are the same as those for other poisonous organophosphorus compounds.

Chemicals

CBDP was a gift from Dr D. Lenz (USAMRICD, Aberdeen PG, MD, USA); this compound is 99.5% pure and was custom synthesized by Starks Associates Buffalo, NY, USA. A 0.1M stock solution of CBDP was made in acetonitrile and stored at −70°C. Working solutions of CBDP were made either in anhydrous methanol, acetonitrile, or dimethylsulfoxide (DMSO) and stored at −70°C. 2-PAM (pralidoxime methiodide, N-methyl-pyridin-1-ium 2-aldoxime methiodide) was Gold-label-grade from Ega-Chemie (Steinheim, Germany) and HI-6 (1-[[[4-(aminocarbonyl) pyridinio] methoxy] methyl]-2-[(hydroxyimino)methyl] pyridinium dichloride monohydrate) was a gift from Dr. D. Genkin (Pharmsynthez, Saint Petersburg, Russia). Water-^{18}O (99 atom % ^{18}O) was from Isotec (a member of the Sigma-Aldrich group St. Louis, MO; cat# 487090). Sequencing grade modified trypsin was from Promega (Madison, WI, cat# V5111). Alpha-cyano-2-hydroxy cinnamic acid (CHCA) was purchased from Fluka (a member of the Sigma-Aldrich group St. Louis, MO, cat# 70990) and prepared as a saturating solution in 50% acetonitrile/water plus 0.3% trifluoroacetic acid. Acetonitrile used for mass spectrometry was DNA sequencing grade from Fisher (Pittsburgh, PA, cat# BP-1170) and trifluoroacetic acid used for mass spectrometry was sequencing grade (> 99.9%) from Beckman (Brea, CA, cat# 290204). All other chemicals were of biochemical grade.

Enzyme sources

Both native and recombinant human BChE (hBChE; accession # P06276) were used in this work. Native hBChE purified from plasma as described (21), was used for the kinetic studies and mass spectrometry. hBChE used for kinetic studies consisted mostly of the tetrameric form. It was 61% pure with an activity of 41 units/ml, using BTC as the substrate at pH 8.0 and 25°C (unit = 1 μmol of substrate hydrolyzed per min). The hBChE that was used for mass spectrometry had an activity of 73,400 units/ml (100 mg/ml), and was >50% pure. Both batches of enzyme were stored for months at +4°C without activity loss in 30 mM Tris/HCl pH 7.5, containing 0.1 M NaCl and 0.02% sodium azide. The recombinant

hBChE was used for crystallization. It was a truncated monomer, containing residues 1–529, and 5 carbohydrate chains rather than the 9 in native hBChE. Recombinant human BChE was expressed in Chinese hamster ovary (CHO) cells and purified by affinity and ion exchange chromatographies, as described previously (22). Its concentration was 6.47 mg/ml. Recombinant human AChE (hAChE; accession #P22303) was expressed in stably transfected Chinese hamster ovary cells (CHO), and purified as described previously (23). Highly purified AChE (>90%) was 300-fold diluted into 0.1 M phosphate buffer pH 8.0 supplemented with 0.1% bovine serum albumin (BSA) and 0.01% sodium azide for all kinetic studies

Enzyme activity and inhibition

Cholinesterase activity was measured by the method of Ellman (24) at pH 8.0, at 25°C in 50 mM phosphate buffer, using acetylthiocholine (ATC) iodide (1 mM) as the substrate for AChE, and butyrylthiocholine (BTC) iodide (1mM) as the substrate for BChE.

Progressive inhibition of enzymes by CBDP was performed in 50 mM sodium phosphate buffer pH 8.0 at 25°C, 10% methanol or 5% acetonitrile. For inhibition studies of hBChE and hAChE, the final CBDP concentrations ranged from 0.5 nM to 10 nM and 0.1 to 5.5 μM respectively. 10% MeOH has no denaturing effect on BChE, and does not alter significantly its reactivity (25,26). Despite the presence of 0.1% BSA, the addition of 10% methanol or 5% acetonitrile caused a decrease in AChE activity that stabilized in a few minutes at 75–80% residual activity. This solvent effect does not interfere with the inhibition mechanism of AChE during the time course of experiments.

Inhibition kinetics were performed under pseudo-first order conditions ([E] ≪ [CBDP]). BChE active site concentration [E] in the inhibition medium was 6×10^{-11} mole/l and AChE active site concentration was 5×10^{-11} mole/l. Enzyme active site concentrations were determined from the catalytic activity of diluted preparations at V_{max}, pH 8.0 and 25°C, taking k_{cat} = 45,500 min^{-1} for BChE with BTC as the substrate (27), and k_{cat} = 400,000 min^{-1} for hAChE with ATC as the substrate (28). The time course of enzyme inhibition was monitored by the Aldridge sampling method i.e. samples were withdrawn at different incubation times (15 sec to 20 min) after addition of CBDP and the remaining enzyme activity was determined. The pseudo-first-order rate constants for adduct formation (k_{obs}) were taken from the slopes of plots of log (residual activity) *versus* time (29,30).

Previous work suggested that initial phosphorylation of the BChE active site serine would lead to a covalent, ring-opened CBDP-serine adduct (1). Covalent adduct formation by CBDP may be described by the classical scheme for reaction of OPs with ChEs (Scheme 2). In this scheme EH stands for the free enzyme, I⊃ for the cyclic phosphotriester CBDP, EH.I⊃ for the noncovalent Michaelis complex between enzyme and CBDP, and EHI for the ring-opened CBDP phosphorylated enzyme. $K_I = k_{-1}/k_1$ is the dissociation constant of complex EH.I⊃, and k_p is the enzyme phosphorylation rate constant. Assuming that rapid equilibrium conditions hold (i.e. $k_p \ll k_{-1}$), the observed rate for inhibition, k_{obs}, is:

$$k_{obs}=\frac{k_p[CBDP]}{K_I+[CBDP]} \quad (1)$$

Analysis of kinetic data was performed using GOSA-fit, a fitting software based on a simulated annealing algorithm (BiogLog, Toulouse, France; http://www.bio-log.biz).

Aging and reactivation of CBDP-inhibited cholinesterases

Reactivation and dealkylation rates for CBDP-phosphonylated ChEs were measured using standard procedure for investigation of oxime-mediated reactivation and aging of ChEs (31). Enzymes were inhibited with CBDP to 95% in less than 15 min, aliquots were removed at various times (from 15 s to 10 min) following inhibition and immediately incubated with oxime reactivators in 0.1 M sodium phosphate buffer pH 8.0 at 25°C. Two different oxime reactivators were tested: 2-PAM (at 1 or 10 mM) and HI-6 (at 0.5 mM). ChE activity was measured as a function of incubation time in the presence of oxime, for up to 24h.

Mass spectrometry of CBDP-inhibited BChE—hBChE was completely inhibited by excess CBDP in the presence and absence of ^{18}O-water. For the reaction in the presence of ^{18}O, 100 μl of ^{18}O-water was combined with 1 μl of 1 M ammonium bicarbonate, 5 μl of BChE (73,400 units/ml) and 1 μl of CBDP (100 mM in acetonitrile). For the reaction in the absence of ^{18}O, 100 μl of ^{16}O-water was combined with 1 μl of 1 M ammonium bicarbonate, 5 μl of BChE (73,400 units/ml) and 1 μl of CBDP (100 mM). The final reaction mixtures contained 56 μM BChE and 930 μM CBDP in 10 mM ammonium bicarbonate. The reactions were incubated at room temperature for 30 minutes, after which time there was no measurable BChE activity remaining (1 μl from each sample was used for measuring activity). Parallel incubations of BChE were made without CBDP. All samples were prepared in siliconized, 1.7 ml, microfuge tubes (Avant from Midwest Scientific, St. Louis, MO, cat# AVSC1510). After the incubations, all four samples were denatured by boiling for 10 minutes, then dried under vacuum in a Savant SpeedVac (Thermo Scientific, Waltham, MA). The purpose for drying was to remove the ^{18}O-water. Removal of the ^{18}O-water before trypsinolysis simplifies interpretation of the mass spectra because trypsin would introduce two ^{18}O-oxygens into the C-terminus of every peptide during proteolysis if trypsinolysis were conducted in an ^{18}O-medium (32). The pellets were redissolved in 106 μl of 10 mM ammonium bicarbonate made with ^{16}O-water. Four μl of sequencing grade trypsin (0.5 μg/μl in 50 mM acetic acid, 200 nmoles of acetic acid) were added to each preparation, followed by 2 μl of 0.1 M ammonium bicarbonate (200 nmoles of bicarbonate) to neutralize the acetic acid. The preparations were incubated at 37°C overnight.

10 μl of each digest were desalted using C18 ZipTips (Millipore, Billerica, MA cat# ZTC18SO96). The ZipTip was wetted with 100% acetonitrile and activated with 0.1% trifluoroacetic acid. One μl of 1% trifluoroacetic acid was added to each 10 μl aliquot of digest. Each acidified digest was loaded onto a separate activated ZipTip, washed with 0.1% trifluoroacetic acid and eluted with 10 μl of 60% acetonitrile/water containing 0.1% trifluoroacetic acid. An aliquot of each eluant was diluted 10-fold with 50% acetonitrile/water plus 0.3% trifluoroacetic acid. Two μl of each dilution were mixed with 2 μl of CHCA (alpha-cyano-4-hydroxycinnamic acid). One μl aliquots of the mixture were spotted onto a MALDI target plate (384-well Opti-TOF plate, cat# 1016491 from Applied Biosystems, Foster City, CA) and allowed to air dry.

Samples were analyzed in a MALDI TOFTOF 4800 mass spectrometer (Applied Biosystems, Foster City, CA) using both reflector positive and reflector negative modes with delayed extraction. Six by 500 laser pulses were accumulated for each measurement, over a mass range of 2000 to 4000 amu, using a laser voltage of 3500 V in positive mode and 3600 V in negative mode. Data collection was controlled by 4000 Series Explorer software (version 3.5). Mass calibration was made with Cal Mix 5 (containing bradykinin, 2–9 clip; angiotensin I; Glu-fibrinopeptide B; adrenocorticotropic hormone [ACTH], 1–17 clip; ACTH, 18–39 clip; and ACTH, 7–38 clip, Applied Biosystems).

Crystallization of recombinant hBChE and generation of the ultimate aged conjugate of CBDP-phosphorylated human BChE

Human BChE was crystallized as described previously (22). The final conjugate of hBChE inhibited by CBDP was obtained by soaking crystals for 12 h in a mother liquor solution (0.1 M MES pH 6.5, 2.1 M ammonium sulfate) containing 1 mM CBDP (at 4°C). The CBDP stock solution was 10 mM in DMSO. Crystals were washed for 5 sec in a cryoprotective solution (0.1 M MES buffer, 2.3 M ammonium sulfate, 20% glycerol) before being flash-cooled in liquid nitrogen for data collection.

X-ray data collection and structure solution of the ultimate aged conjugate of CBDP-phosphoryated human BChE

Diffraction data were collected at the European Synchrotron Radiation Facility (ESRF, Grenoble, France). Data for crystalline hBChE inhibited by CBDP were collected at 100K, on the ID14-eh4 beam line using $\lambda = 0.9765$ Å wavelength with an ADSC Quantum Q315r detector (33). The data set was processed with XDS (34) and the structure was solved with the CCP4 suite (35). An initial model was determined by molecular replacement with MolRep (36), starting from the recombinant hBChE structure (PDB entry 1P0I) from which all ligands and glycan chains were removed. The initial model was refined as follows: a rigid-body refinement, made with REFMAC5 (37), was followed by iterative cycles of model building with Coot (38), and then restrained and TLS refinement was carried out with REFMAC5 (39). TLS groups were defined with the help of the *TLS Motion Determination* server (http://skuld.bmsc.washington.edu/~tlsmd/index.html) (40). The bound ligand and its descriptions were built using the Dundee PRODRG2.5 server including energy minimization using GROMOS96.1 force field calculations.

Results and discussion

Kinetics for the inhibition of human cholinesterases by CBDP

Inhibition of BChE by CBDP did not follow simple first-order progressive kinetics. Plots of residual activity ($Ln(A/A_0)$ *versus* time were biphasic, despite the fact that the basic condition for a first-order reaction was maintained, i.e. the enzyme concentration in the reaction medium was much less than the CBDP concentrations, and that CBDP was stable during the course of inhibition. In addition, titration experiments with [CBDP] varying from 0.2 [E_0] to 0.9 [E_0] showed that there was no spontaneous reactivation of inhibited enzymes. Thus, the biphasic progressive inhibition can be regarded as the sum of two first-order processes, a fast phase and a slow phase. It should be noted that the first-order lines for both phases extrapolated to Ln50% activity at t=0. Situations similar to this - where first-order lines do not pass through the origin - were described by Aldridge and Reiner (30). In one case, they described partial inhibition at zero-time i.e. rapid equilibrium formation of an inhibitory complex prior to phosphonylation. In another case, there was ‘ongoing’ inhibition during the reaction with substrate (41–43). These situations could be identified by of dilution of the enzyme prior to measurement of residual activity or by increasing the substrate concentration during activity measurement. Neither dilution of inhibited enzyme prior to measurement of residual activity, nor increasing the concentration of substrate ([BTC] from 0.25 mM to 10 mM) during assay changed the extrapolated Ln(% activity) of BChE. These observations indicate that neither ‘ongoing’ inhibition or rapid equilibrium binding of inhibitor are responsible for the biphasic inhibition behavior exhibited by CBDP. In addition, for the type of behavior described by Aldridge and Reiner (30) and Estevez and Vilanova (41), the intercept on the activity axis depends on inhibitor concentration. In the case of inhibition of BChE by CBDP, first-order lines for the slow phase extrapolated through the ordinate at [E_0]=50±10% regardless [CBDP]. After subtraction of the slow process contribution, the first-order lines for the fast phase also extrapolated through the

ordinate at [E′$_0$]=50±10% whatever [CBDP]. The sum of the two ordinate intercepts was always equal to 100%. Both fractional activities at t_0 may be regarded as the relative activities of two enzyme forms. Since both fractional activities are the same, the two enzyme forms are present in the preparation in similar amounts. Inhibition of AChE by CBDP is also biphasic. However, in this case, the extrapolated y-axis intercept for the fast phase is larger than the extrapolated intercept for the slow phase. Therefore the fast phase form of AChE, [E′$_0$], is present in higher concentration than the slow phase form, [E$_0$].

The biphasic progressive inhibition indicates that CBDP reacts at different rates with two different active populations of butyrylcholinesterase (E and E′) that are in slow equilibrium (44.45). The affinity of both forms for certain inhibitors can be different and their reactivity can be different too. Such an inhibition pattern has also been observed for carbamylation of BChE with, N-methyl-N-(2-nitrophenyl) carbamoyl chloride (46). This situation is described in Scheme 3. Thus, the kinetics for inhibition of ChEs by CBDP, under pseudo-first order conditions, can be described by the following equation:

$$[E]_t=[E]_0e^{-k_{obs}\cdot t}+[E']_0e^{-k'_{obs}\cdot t} \quad (2)$$

with $k_{obs}>k'_{obs}$, and,

$$[E_{tot}]_0=[E]_0+[E']_0,\ k_{obs}=\frac{k_p\cdot[I]}{K_I+[I]},\ k'_{obs}=\frac{k'_p\cdot[I]}{K'_I+[I]},\ K_I=\frac{k_{off}}{k_{on}} \text{ and } K'_I=\frac{k'_{on}}{k'_{off}} \quad (3)$$

By convention we refer to k_{obs} for the fast phase and to k'_{obs} for the slow phase. Fig. 1 shows typical biphasic plots for progressive inhibition of BChE by CBDP that fit with equation 2. Measured values for k_{obs} and k'_{obs} are calculated by non linear regression fit using equation 2.

For BChE, replots of k_{obs} versus [CBDP] for both the fast and slow phases were linear, passing through the origin (Fig. 1, insert). This indicates that for both the E and E′ forms of BChE, the highest CBDP concentration (10 nM) remained lower than K_I and K'_I. It follows that under our experimental conditions, k_{obs} and k'_{obs} reduce to:

$$k_{obs}=\frac{k_p}{K_I}[I]=k_i\cdot[I] \text{ and } k'_{obs}=\frac{k'_p}{K'_I}[I]=k'_i\cdot[I] \quad (4)$$

With k_i and k'_i the bimolecular rate constants of the inhibition. Determined values of k_i and k'_i are given in Table 1.

The situation was somewhat different for AChE (data not shown). The inhibition kinetics were biphasic and a replot of the slow phase k'_{obs} versus [CBDP] was linear and passed through the origin. The linear dependence of k'_{obs} on [CBDP] indicates that, as for BChE, the highest experimental CBDP concentration (5.5 μM) was far less than K'_I. However, the fast phase of inhibition was independent of the CBDP concentration, giving k_{obs}=0.37±0.15 min^{-1}. Such a situation occurs if the CBDP concentration is very much larger than K_I, so that k_{obs} reduces to k_p, i.e. the E form is saturated by CBDP even at the lowest concentration (0.1 μM).

Determined values of k'_i for inhibition of AChE form E′ under different solvent conditions are also given in Table 1. Experimental values remain in the same order of magnitude showing that the solvent effect is weak. The slight increase in k'_i observed for inhibition performed in 5% acetonitrile may reflect a specific effect of this solvent on AChE as it has been reported by several investigators (47), but did not reflect a change in the mechanism of inhibition.

The determined values of the bimolecular rate constants for phosphonylation of both hBChE (k_i=1.5±0.2×10^8 and k'_i=2.5±0.7×10^7 $M^{-1}min^{-1}$) and hAChE (>3.7×10^6 and 1.06±0.23×10^5 $M^{-1}min^{-1}$) by CBDP (Table 1) are much faster than values previously reported for inhibition of cholinesterase by CBDP. Maxwell obtained a value of 1.1×10^3 $M^{-1}min^{-1}$ for rat brain AChE at pH 7.4 and 37° C (14). Cohen found a value of 2.1×10^3 $M^{-1}min^{-1}$ for recombinant human AChE and 2×10^4 $M^{-1}min^{-1}$ for human BChE at pH 8.0 and 27°C (20). The major difference between those experiments and ours is that those authors used CBDP stock solutions that were made in aqueous buffer. The problem with aqueous solutions of CBDP is that CBDP is unstable in water. We found that the hydrolysis rate of CBDP in 0.1M sodium phosphate pH 8.0 was 0.0126 min^{-1} at 25°C, i.e. $t_{1/2}$ = 55 min. This agrees with a previously reported $t_{1/2}$ value of 60 min in 36 mM barbiturate-8mM potassium phosphate buffer pH 8.0 (6). Saligenin-derived, six-membered cyclic phosphates (oxon) are even more sensitive to hydrolysis (48). Instability of these compounds is reported to be due to strain in the distorted benzodioxaphosphorin ring (49,50).

Our results (Table 1, k'_i in 10% MeOH) show that the slow phase reactivity of hBChE (form E′) with CBDP is 235±110-fold faster than the reactivity of hAChE (form E′). Though it was not possible to determine k_i for hAChE (form E) directly, an estimate could be made from the following. The k_p for BChE (form E) can be estimated from its k_i, knowing from the experiments that K_I for BChE must be much larger than 10 nM. Since k_i for BChE is 1.5×10^8 $M^{-1}min^{-1}$ and $K_I \gg$ 10 nM, then $k_p=k_i.K_I$ for BChE $\gg$ 1.5 min^{-1} > 0.37 min^{-1} = k_p for AChE. So on the one hand we know that k_p for BChE $\gg$ k_p for AChE, and on the other hand, we don't expect that K_I for AChE is smaller than that for BChE, because the active site of AChE poorly accommodates large ligands like CBDP compared to the active site of BChE. It follows that k_i for AChE (form E) $\ll$ k_i for BChE, i.e. the reactivity of AChE (form E) is much lower than the reactivity for BChE (form E).

However, a lower limit value for k_i for AChE (fast form, E) may be estimated from the experimental value of k_p = 0.37 min^{-1} and $K_I \ll$ 0.1 μM giving $k_i \gg$ 3.7×10^6 $M^{-1}min^{-1}$. Despite the reactivity of AChE with CBDP being lower than that of BChE, it appears to be larger than some nerve agents like tabun (7.4×10^6 $M^{-1}min^{-1}$) (51).

Aging and non-reactivatibility of CBDP-inhibited BChE

Previous MALDI-TOF mass spectral studies suggested that two post-inhibitory reactions occurred after formation of the initial BChE covalent adduct, i.e. rapid hydrolysis of the ring-opened CBDP adduct into an o-cresyl-phospho-serine adduct with release of saligenin, followed by conversion of this adduct into a phospho-serine adduct plus o-cresol (1) (Scheme 4). Both dealkylation steps can be considered aging steps.

It is generally accepted that oximes can reactivate the initial, covalent adduct of organophosphate inhibited cholinesterases, but that after aging, oxime reactivation is ineffective. In order to determine how fast the CBDP aging reactions occur, we measured oxime-mediated reactivation of CBDP-inhibited BChE and AChE.

Attempts to reactivate both CBDP-phosphonylated AChE and BChE by oximes 2-PAM and HI-6 failed. Experiments were performed in triplicate. This strongly suggests that aging is

very rapid after inhibition by CBDP. The kinetics indicated that loss of reactivatibility occurs in less than 15 s following inhibition. Aging of α-chymotrypsin (52) and fly AChE (19) inhibited by CBDP was also found to be very rapid. These enzymes were not reactivatable even with strong nucleophilic compounds. A previous mass spectrometry study of human albumin phosphonylated by CBDP indicated that a rapid, water-mediated loss of saligenin occurred after phosphonylation (1). This reaction occurred despite the fact that albumin adducts of other organophosphates do not age at all (53). A mass spectral study of the human BChE-CBDP adduct indicated that two consecutive post-phosphorylation reactions occur: a rapid loss of saligenin was followed by loss of the cresyl moiety, leading to a phospho-serine adduct (1). Our kinetic results confirm the rapidity of the first post-inhibitory reactions of CBDP-phosphonylated BChE and CBDP-phosphonylated AChE to form aged adducts, and illustrate the difficulties in reactivating such aged enzymes.

Mass spectrometry

Following the formation of the initial reaction of CBDP with BChE, there are two adduct modifications (Scheme 4) (1). The initial ring opened adduct is not seen with BChE, but its presence can be inferred by analogy with the reactions of other OP with BChE and from a similar nucleophilic reaction between CBDP and tyrosine (1). The dealkylation reactions that follow the initial adduct formation involve hydrolysis of the P-O-C linkage. The question to be addressed by the ^{18}O-mass spectral experiments is whether the P-O bond or the O-C bond is cleaved during the course of these dealkylation reactions.

If the P-O bond is cleaved in a medium containing ^{18}O-water, then an ^{18}OH will be added to the phosphorus; but if the O-C bond is cleaved, then the ^{18}OH will be added to the carbon and the original ^{16}O will remain on the phosphorus. Exchange of ^{18}O for ^{16}O can be discerned by a 2 amu increase in mass of the phospho(organophospho)-peptide adduct. MALDI TOF mass spectral analysis of tryptic digests from BChE reacted with CBDP in the presence ^{18}O-water or in the presence of ^{16}O-water are shown in Figure 2 (panels A, B, E, F, I, and J). The results are compared to tryptic digests of BChE incubated under the same conditions without CBDP (Figure 2; panels C, D, G, H, K, and L). Limited mass ranges are presented in order to illustrate the isotopic splitting for the masses of interest, and to reduce interference from more intense signals. Spectra in panels A, B, C, and D show the mass of the unlabeled active site peptide from BChE, SVTLFGESAGAASVSLHLLSPGSHSLFTR, taken in positive reflector mode. The theoretical, protonated $[M+H]^{+1}$, monoisotopic mass of this peptide is 2928.52 amu (obtained with the assistance of the MS-Product algorithm from Protein Prospector at http://prospector.ucsf.edu/prospector). Spectra in panels E, F, G, and H show the mass of the phospho adduct of the active site peptide taken in negative reflector mode. The theoretical, deprotonated $[M-H]^{-1}$, monoisotopic mass of this peptide is 3006.52 amu in negative mode. Spectra in panels I, J, K, and L show the mass of the cresyl-phospho adduct of the active site peptide taken in negative reflector mode. The theoretical, deprotonated $[M-H]^{-1}$, monoisotopic mass of this peptide is 3096.52 amu. Negative mode spectra of the phospho-adducts showed better resolution and better signal-to-noise than spectra in positive mode, despite the fact that the signal intensities were greater in positive mode.

The unlabeled active site peptide produced by digestion in either ^{18}O- or ^{16}O-media gave identical spectra with a monoisotopic, $[M+H]^{+1}$ mass of 2928.27±0.08 amu (Figure 2, panels C and D), indicating that spontaneous exchange of ^{18}O into the peptide did not occur. The 1 amu isotopic splitting and the isotopic pattern of this family of peaks are consistent with a mass of 2928 amu (the isotopic pattern was checked with the MS-Isotope algorithm from Protein Prospector at http://prospector.ucsf.edu/prospector). Weak, unresolved spectra in the vicinity of 2928 amu were seen in the digests from the CBDP-containing samples (Figure 2, panels A and B), despite the fact that CBDP had inhibited all of the BChE

activity. The unresolved character of these spectra indicates that these masses arose in the MALDI TOF mass spectrometer from fragmentation in the flight path after the reflector.

The cresyl-phospho adducts from the CBDP reactions conducted in the presence of either ^{18}O- or ^{16}O-media gave identical spectra with a monoisotopic, $[M-H]^{-1}$ mass of 3096.15±0.05 amu (Figure 2, panels I and J), indicating that oxygen from the medium was not added to the phosphorus during hydrolysis of the saligenin. This in turn indicates that O-C bond fission accompanied this hydrolysis. This sort of dealkylation is characteristic of aging in BChE (54). Aging is assisted by groups in the pi-cation binding pocket of the active site (55,56) and is specific for the ligand bound into this pocket (23,24,57,58). This suggests that for the initial, ring-opened adduct the saligenin moiety is bound into the pi-cation binding pocket. The 1 amu isotopic splitting and the isotopic pattern of this family of peaks support the argument that these signals are a genuine reflection of a monoisotopic 3096 amu mass. Absence of signal at 3096 amu from the digests of BChE incubated without CBDP (Figure 2, panels K and L) indicates that the 3096 signal is a characteristic of the CBDP reaction and is not an adventitious mass occurring in the BChE tryptic digest.

The phospho adduct from the reaction of BChE with CBDP in the presence ^{18}O-water gave a mass of 3008.23 amu, whereas the same reaction in ^{16}O-water resulted in a mass of 3006.09 (Figure 2, panels E and F). Since the theoretical mass for the phosphorylated active site peptide in negative mode is 3006.51 amu, the 3008.23 amu mass from the ^{18}O-reaction indicates that one oxygen atom from the medium was added to the phosphorus during hydrolytic release of the cresyl. This in turn indicates that the P-O bond was broken during this hydrolysis. P-O bond breakage is consistent with the cresyl moiety being located in the acyl binding pocket where the classical aging type of assistance for fission of the O-C bond is unavailable. The 1 amu isotopic splittings and the isotopic patterns of these two families of peaks support the argument that these signals are genuine reflections of monoisotopic masses at 3006 and 3008 amu. The absence of signal in the 3006–3008 amu region from the digests from BChE incubated without CBDP (Figure 2, panels G and H) indicates that the 3006 and 3008 amu signals are characteristic of the CBDP reaction and are not adventitious masses occurring in the BChE tryptic digest.

X-ray structure of phospho-hBChE

The structure of CBDP inhibited-hBChE after 12 hours of soaking was solved at 2.3 Å of resolution. Data and refinement statistics are shown in Table 2. In the experimental |Fo|−|Fc| electron density map, a strong positive peak is observed (above 15σ) at covalent bonding distance of the catalytic Ser198 confirming the presence of the phosphorus atom. The structure was unambiguously refined as a phospho-serine adduct, indicating the departure of both o-cresyl and saligenin substituents after 12 hours of incubation (Figure 3).

In the structure of BChE phosphoserine adduct the phosphorus atom of the phosphate adduct is at 1.8 Å from Ser198Oγ. The oxygen O_2 of the phosphate adduct is negatively charged and forms a salt bridge with the catalytic histidine His438Nε2 (2.9 Å). The oxygen Oδ is stabilized by H-bonding with atoms from residues forming the oxyanion hole, Gly116N (2.7 Å), Gly117N (2.6 Å), and Ala199N (2.7 Å). The O_3 is oriented toward the acyl-binding pocket and interacts with water molecule w 100 (3.3 Å) stabilized by H-bond interaction with the main chain oxygen of the Leu286 (3.1 Å). The choline-binding pocket is occupied by water molecules (w125, w 103) at equal distance of the Trp82 and the oxygen O_2 of CBDP adduct (approximately 4 Å). This crystal structure confirmed the formation of a phospho-serine adduct resulting from two consecutive post-phosphorylation reactions of the ring opened CBDP adduct in the hBChE active site.

This is the first time that a phosphoserine has been observed as the final conjugate from the reaction of BChE with an OP. A phosphoserine adduct resulting from dealkylation of human AChE inhibited by the phosphoramidate mipafox was already reported (59). Evidence for this adduct was based on mass spectrometry and immuno-precipitation of trypsin digests with monoclonal antibodies to phosphoserine. Our previous studies with phosphoramidates (tabun and tabun derivatives) showed that for phosphoramidates, displacement of isopropyl amine groups results from acid hydrolysis during sample preparation for mass spectrometry (23). Thus, although mass spectrometry alone does not provide absolute evidence for non-artefactual formation of phosphoserine adduct, immuno-precipitation of trypsin digests rules out possible artefactual acid-induced formation of this adduct. In our study, x-ray analysis of CBDP-aged BChE adduct provides direct and 3D evidence that the phosphoserine adduct does not result from sample preparation, but results from post-phosphorylation chemical events. Interestingly, both CBDP-phosphorylated human BChE and AChE (Carletti et al., in preparation) lead to phosphoserine adducts while only mipafox-inhibited AChE leads to phosphoserine adduct. With BChE, the mipafox-aged adduct is a monoisopropylphosphoroamido adduct (60).

Concluding remarks

Kinetics and mechanism

With k_i values of 10^7–10^8 M^{-1} min^{-1}, CBDP is one of the most potent OP inhibitors yet found for BChE. Comparable reactivities are seen with cyclosarin (3.8×10^8 M^{-1} min^{-1}) (61), FP-biotin (1.6×10^8 M^{-1} min^{-1}) (62), diazoxon (7.7×10^7 M^{-1} min^{-1}) (62), and soman (5.1×10^7 M^{-1} min^{-1}) (63). Only chlorpyrifos-oxon (1.7×10^9 M^{-1} min^{-1}) (64) and MEPQ (6.3×10^8 M^{-1} min^{-1}) (63) are appreciably more reactive. Thus, BChE should be a sensitive marker of low level exposure to CBDP.

The ultimate product of the reaction of CBDP with BChE (and with AChE) is a unique phosphopeptide not previously reported for reaction of OP with BChE. This phosphopeptide is the result of two consecutive, post-phosphorylation reactions (aging), starting from the CBDP ring-opened adduct (see Scheme 4). The first reaction involves hydrolysis of the O-C bond in the P-O-C linkage between the phosphorus and the saligenin moiety, which is indicated by the observation that oxygen from the medium is not added to the phosphorus.

Fission of the O-C bond is characteristic of enzyme assisted “aging” for phosphylated BChE adducts (54). Aging involves phosphorus-ligands located in the pi-cation binding site (i.e. near Trp82 in hBChE, Trp87 in hAChE) (23,57,58).

This argues that the saligenin moiety probably occupied the choline-binding site in the initial ring-opened form of the CBDP adduct, suggesting in turn that the o-cresyl substituent occupied the acyl-binding pocket of hBChE.

Based on chemical analyses, Toia and Casida (52) proposed a similar dealkylation process for chymotrypsin and trypsin inhibited by saligenin cyclic phosphonates and phosphates. In addition to release of saligenin from the phosphorus into the medium, they proposed that a portion of the saligenin released from the phosphorus was trapped by the active site histidine. No evidence for a similar trapping of the released saligenin was seen for either AChE or BChE adducts of CBDP.

The second reaction involves hydrolysis of the P-O bond between the phosphorus and the cresyl moiety. Cleavage of the P-O bond is indicated because oxygen from the solvent is added to the phosphorus during this reaction. Fission of the P-O bond is consistent with either a dissociative (SN1) hydrolysis of phosphoesters or a nucleophilic (S_N2) hydrolysis

(65). An S_N2 was earlier suggested as one of two alternative mechanisms for aging of diethylphosphoryl-BChE (66). But it was later discarded in favor of a dealkylation-based mechanism because no incorporation of ^{18}O-water to the phosphorus was found by mass spectrometry analysis. However, structural analysis of the aging of some analogues of the nerve agent tabun suggested a S_N2 based mechanism (67). A S_N2 mechanism requires that the nucleophile (in this case water) approach the phosphorus from the face of the tetrahedral phosphate structure that is opposite from the group to be displaced. This face is accessible to water after departure of saligenin substituent in the previous step. The dissociative mechanism requires that the leaving group (in this case the cresyl) detach from the phosphorus and depart to make room for the replacing group (in this case water) to attach. At this point the data do not allow discriminating between an S_N1 or S_N2 mechanism. The complete inhibition mechanism by CBDP up to the formation of the phosphoserine is summarized in Scheme 5.

Aerotoxic syndrome and toxicity of CBDP

Aerotoxic syndrome is speculated to be asociated with exposure to tri-ortho-cresylphosphate, but this association has not been proven. After exposure to TOCP, the CBDP generated *in vivo* can react with tissue enzymes such as liver carboxylesterase and neuropathy target esterase (NTE), and with blood bioscavengers such as albumin and BChE (note that CBDP does not react with paraoxonase 1, the naturally-occurring plasma phosphotriesterase, Masson et al., unpublished results). Detection of low dose exposure to CBDP is critical to ongoing investigations into aerotoxic syndrome. It is suspected that aerotoxic syndrome is caused by internalization of an engine oil additive (TOCP) that gives rise to CBDP *in vivo*. Epidemiological studies into aerotoxic syndrome are currently hamstrung by the absence of a direct, quantitative, *in vivo* measure for exposure to TOCP. Phosphorylated BChE, as a biomarker for TOCP/CBDP exposure, is an appealing candidate to fill this vacancy. The unique nature of this adduct will reduce the incidence of false positive identifications when screening populations.

Use of a phosphorylated protein as a biomarker for aerotoxic syndrome entails the potential for conflict with other phosphorylated proteins, of which there are many. However, ongoing work in our laboratory has demonstrated that phosphorylated BChE (partially purified from serum by anion exchange and procainamide affinity chromatography to give 15–30% pure BChE) yields a phosphorylated peptic peptide that is specific for the active-site sequence of BChE (manuscript submitted). This peptide is readily detectible by MALDI TOF TOF mass spectrometry and its identity has been confirmed by mass spectral fragmentation analysis. It provides a unique biomarker for reaction of CBDP with BChE. We have used this peptide marker to address the question of whether there is sufficient cresyl phosphate in aircraft cabin air to cause detectible adduct formation in passengers. This question is at the heart of the debate between expert bodies on the extent of potential exposure to and the toxic potency of cresyl phosphate. To date, we have found that about half of the passengers tested carried evidence for exposure to TOCP despite the fact that none of the subjects were exposed to high levels of engine gases (i.e. a “fume event”) and none reported toxic symptoms. Since only a sub-group of passengers experience aerotoxic symptoms after a “fume event” it can be concluded that some individuals are hyper-sensitive to the toxicants in the engine fumes. Evidence for TOCP toxicant in a substantial fraction of passengers exposed to normal cabin air provides ample reason to suspect that the level of TOCP in aircraft air (however small it may be) is a potential threat to sensitive passengers exposed to “fume events”.

The high reactivity of BChE toward CBDP also argues that it should play an important role in natural defenses against toxicity from low dose exposure to TOCP by scavenging CBDP from the blood stream. Variation in the reactivity of BChE or cytochrome P450 enzymes

due to naturally occurring mutations or diseases (68) may contribute to the explanation for why only selected passengers and aircraft workers fall victim to aerotoxic syndrome

The initial neurological symptoms associated with aerotoxic syndrome are similar to symptoms associated with organophosphate inhibition of AChE. Though AChE is less reactive than BChE with CBDP, the reactivity of AChE with CBDP is similar to reactivity with potent OPs like paraoxon ($k_i \approx 10^6\ M^{-1}.min^{-1}$) or (−)-tabun ($k_i \approx 2.7\times10^7\ M^{-1}.min^{-1}$) (69), suggesting that human exposure to high doses of CBDP should cause typical symptomatology of OP poisoning. Neurotoxicity that persists for years suggests targets in addition to AChE.

Origin of aerotoxic syndrome and organophosphate-induced delayed neuropathy

Aerotoxic syndrome is assumed to be caused by exposure to low doses of TOCP (2). Organophosphate-induced delayed neuropathy (OPIDN) is known to be caused by exposure to high doses of TOCP (10,70, 71,72). High doses of TOCP result in paralysis of the legs, whereas low doses do not cause delayed paralysis. The processes leading to OPIDN and the long-term symptoms of aerotoxic syndrome are probably related. A long-standing candidate for the target of CBDP responsible of the induction of OPIDN is neuropathy target esterase (NTE), a membrane bound phospholipase that catalyzes the deacylation of membrane-phophatidylcholine to soluble glycerophosphocholine and fatty acids (73,74, 75). Low doses of TOCP inhibit neuropathy target esterase, though they do not cause neuropathy. A role for NTE in delayed neuropathy is supported by the finding that human genetic variants of NTE have motor neuron disease characterized by spastic paraplegia and distal muscle wasting (76,77). Proposed noncholinergic mechanisms of OP neurotoxicity include activation of glutamatergic neurons, and oxidative damage from reactive oxygen species and from peroxynitrite radicals (78). The recent discovery that OP can covalently modify amino acid residues other than the traditionally-accepted active site serines of serine esterases/proteases has fueled interest in non-traditional targets for OP. The covalent modification of tyrosine residues by OP on non-enzymatic proteins such as serum albumin and tubulin, both *in vitro* (79) and *in vivo* (80), and with lysine residues (81) opens the possibility for direct alteration of non-enzymatic, structural and connective proteins in the neuron that could lead to degradation of function and the slow development of the long term neurological symptoms associated with aerotoxic syndrome and organophosphate-induced delayed neuropathy.

Acknowledgments

Funding Support

This work was supported by U.S. Army Medical Research and Materiel Command [W81XWH-07-2-0034 to OL]; National Institutes of Health [U01 NS058056 to OL, P30CA36727 to Eppley Cancer Center]. Mass spectra were obtained with the support of the Mass Spectrometry and Proteomics core facility at the University of Nebraska Medical Center. We are grateful to the ESRF for beam-time under long-term projects MX498, MX609 and MX722 (IBS BAG) and MX551 and MX 666 (radiation-damage BAG) and the ESRF staff for providing efficient help during data collection. Financial support by the CEA, the CNRS and the UJF is acknowledged, as well as a grant to MW and FN from the Agence Nationale de la Recherche (ANR; project number ANR-09-BLAN-0192-04) and to MW from the DGA (project number DGA-REI 2009-34-0023).

We thank Dr D. Lenz (USAMRICD, Aberdeen PG, MD, USA) for the gift of CBDP and Dr D. Genkin (Pharmsynthez, Saint Petersburg, Russia) for the gift of HI-6 dichloride.

Abbreviations

AChE	acetylcholinesterase, EC 3.1.1.7
ATC	acetylthiocholine

BChE	butyrylcholinesterase, EC. 3.1.1.8
BSA	bovine serum albumin
BTC	butyrylthiocholine
CBDP	2-(o-cresyl)-4H-1,3,2-benzodioxaphosphoran-2-one (or CSP; cresyl saligenin phosphate)
ChE	cholinesterase
CHCA	alpha-cyano-4-hydroxycinnamic acid
CHO	Chinese hamster ovary
DMSO	dimethylsulfoxide
HI-6	1-[[[4-(aminocarbonyl) pyridinio] methoxy] methyl]-2-[(hydroxyimino)methyl] pyridinium dichloride monohydrate
hAChE	human AChE
hBChE	human BChE
MALDI-TOF	matrix-assisted laser desorption/ionization-time of flight
NTE	neuropathy target esterase
OP	organophosphorus compound
OPIDN	organophosphate-induced delayed neuropathy
2-PAM	pralidoxime methiodide, N-methyl-pyridin-1-ium 2-aldoxime methiodide
TCP	tricresyl phosphate
TOCP	tri-ortho-cresyl phosphate

References

1. Schopfer LM, Furlong CE, Lockridge O. Development of diagnostics in the search for an explanation of aerotoxic syndrome. Anal Biochem. 2010; 404:64–74. [PubMed: 20447373]
2. Brown MA, Brix KA. Review of health consequences from high-, intermediate- and low-level exposure to organophosphorus nerve agents. J Appl Toxicol. 1998; 18:393–408. [PubMed: 9840747]
3. Kidd JG, Langworthy OR. Jake paralysis: paralysis following the ingestion of Jamaica ginger extract adulterated with tri-ortho-cresyl phosphate. Bull Johns Hop Hosp. 1933; 52:39–65.
4. Smith HV, Spalding JMK. Outbreak of paralysis in Morocco due to ortho-cresyl phosphate poisoning. Lancet. 1959:1019–1021. [PubMed: 13831987]
5. Casida JE, Eto M, Baron RL. Biological activity of a tri-o-cresyl phosphate metabolite. Nature. 1961; 191:1396–1397. [PubMed: 13877086]
6. Eto M, Casida JE, Eto T. Hydroxylation and cyclization reactions envolved in the metabolism of tri-o-cresyl phosphate. Biochem Pharmacol. 1962; 11:337–352. [PubMed: 13890904]
7. Eto M, Oshima Y, Casida JE. Plasma albumin as a catalyst in cyclization of diaryl o-(α-hydroxy)tolyl phosphate. Biochem Pharmacol. 1967; 16:295–308. [PubMed: 6029915]
8. De Nola G, Kibby J, Mazurek W. Determination of *ortho*-cresyl phosphate isomers of tricresyl phosphate used in aircraft turbina engine oils by gas chromatography and mass spectrometry. J Chromatogr A. 2008; 1200:211–216. [PubMed: 18550071]
9. Winder C, Balouet JC. The toxicity of commercial jet oils. Environ Res. 2002; 89:146–164. [PubMed: 12123648]
10. Winder C. Hazardous chemicals on jet aircraft: cases study- jet engine oils and aerotoxic syndrome. Curr Top Toxicol. 2006; 3:65–88.

11. Van Netten C, Leung V. Hydraulic fluids and jet engine oil: pyrolysis and aircraft air quality. Archiv Environ Health. 2001; 56:181–186.
12. Clement JG. Importance of aliesterase as a detoxification mechanism for soman (Pinacolylmethylphosphonofluoridate) in mice. Biochem Pharmacol. 1984; 33:3807–3811. [PubMed: 6508835]
13. Maxwell DM, Brecht KM, o'Neill BL. The effect of carboxylesterase inhibition on interspecies differences in soman toxicity. Toxicol Lett. 1987; 39:35–42. [PubMed: 3672554]
14. Maxwell DM. The specificity of carboxylesterase protection against the toxicity of organophosphorus compounds. Toxicol Appl Pharmacol. 1992; 114:306–312. [PubMed: 1609424]
15. Glynn P. Neuropathy target esterase. Biochem J. 1999; 344:625–663. [PubMed: 10585848]
16. Boskovic B. The influence of 2-/o-cresyl/-4 H-1:3:2-benzodioxa-phosphorin-2-oxide (CBDP) on organophosphate poisoning and its therapy. Arch Toxicol. 1979; 42:207–216. [PubMed: 475595]
17. Cohen O, Kronman C, Raveh L, Mazor O, Ordentlich A, Shafferman A. Comparison od polyethylene glycol-conjugated recombinant human acetylcholinesterase and serum human butyrylcholinesterase as bioscavengers of organophosphate compounds. Mol Pharmacol. 2006; 70:1121–1131. [PubMed: 16801396]
18. Eto M. Development of insecticidal cyclic phosphoryl compounds through chemical and biochemical approaches. J Environ Sci Health. 1983; B18:119–145.
19. Shiotsuki T, Eto M. Effect of salioxon and fenitroxon on altered acetylcholinesterase of organophosphate-resistant housefly. J Pesticide Sci. 1987; 12:17–21.
20. Hirashima A, Ishaaya I, Ueno R, Ichiyama Y, Wu SY, Eto M. Biological activity of optically active salithion and salioxon. Agric Biol Chem. 1989; 53:175–178.
21. Lockridge O, Schopfer LM, Winger G, Woods GH. Large scale purification of butyrylcholinesterase from human plasma suitable for injection into monkeys; a potential new therapeutic for protection against cocaine and nerve agent tocicity. J Med CBR Def. 2005; 3 on line.
22. Nachon F, Nicolet Y, Viguié N, Masson P, Fontecilla-Camps JC, Lockridge O. Engineering of a monomeric and low-glycosylated form of human butyrylcholinesterase: expression, purification, characterization and crystallization. Eur J Biochem. 2002; 269:630–637. [PubMed: 11856322]
23. Carletti E, Li H, Li B, Ekström F, Loiodice M, Gillon M, Froment MT, Lockridge O, Schopfer LM, Masson P, Nachon F. Aging of cholinesterases phosphylated by tabun proceeds through O-dealkylation. J Am Chem Soc. 2008; 130:16011–16020. [PubMed: 18975951]
24. Ellman GL, Courtney KD, Andres V, Featherstone RM. A new and rapid colorimetric determination of acetylcholinesterase activity. Biochem Pharmacol. 1961; 7:88–95. [PubMed: 13726518]
25. Whittaker M. The pseudocholinesterase variants. Differentiation with n-butyl alcohol: recognition of new phenotypes. Acta Genet Statist Med. 1968; 18:325–334.
26. Ferro A, Masson P. Kinetic evidence for thermally induced conformational change of butyrylcholinesterase. Biochim Biophys Acta. 1987; 916:193–199. [PubMed: 3676330]
27. Grunwald J, Marcus D, Papier Y, Raveh L, Pittel Z, Ashani Y. Large-scale purification and long-term stability of human butyrylcholinesterase: a potential bioscavenger drug. J Biochem Biophys Meth. 1997; 34:123–135. [PubMed: 9178088]
28. Ordentlich A, Barak D, Kronman C, Ariel N, Segall Y, Velan B, Shafferman A. Contribution of aromatic moieties of tyrosine 133 and of the anionic subsite tryptophan 86 to catalytic efficiency and allosteric modulation of acetylcholinesterase. J Biol Chem. 1995; 270:2082–2091. [PubMed: 7836436]
29. Kitz R, Wilson IB. Esters of methanesulfonic acid as irreversible inhibitors of acetylcholinesterase. J Biol Chem. 1962; 237:3245–3249. [PubMed: 14033211]
30. Aldridge WN, Reiner E. Acetylcholinesterase: two types of inhibition by an organophosphorus compound: one the formation of phosphorylated enzyme and the other analogous to the inhibition by substrate. Biochem J. 1969; 115:147–162. [PubMed: 5378376]
31. Masson P, Fortier PL, Albaret C, Froment MT, Bartels CF, Lockridge O. Aging of di-isopropyl-phosphorylated human butyrylcholinesterase. Biochem J. 1997; 327:601–607. [PubMed: 9359435]

32. McCarthy AA, Brockhauser S, Nurizzo D, Theveneau P, Mairs T, Spruce D, Guijarro M, Lesourd M, Ravelli RB, McSweeney S. A decade of user operation on the macromolecular crystallography MAD beamline ID 14–4 at the ESRF. J Synchrotron Radiat. 2009; 16:803–812. [PubMed: 19844017]
33. Yao X, Freas A, Ramirez J, Demirev PA, Fenselau C. Proteolytic 18O labeling for comparative proteomics: model studies with two serotypes of adenovirus. Anal Chem. 2001; 73:2836–2842. [PubMed: 11467524]
34. Kabsch W. XDS. Acta Crystallogr, Sect D: Biol Crystallogr. 2010; 66:125–132. [PubMed: 20124692]
35. Collaborative-Computational-Project4. The CCP4 suite: programs for protein crystallography. Acta Crystallogr D Biol Crystallogr. 1994; 50(Pt 5):760–763. [PubMed: 15299374]
36. Vagin A, Teplyakov A. MOLREP: an automated program for molecular replacement. J Appl Crystallogr. 1997; 30:1022–1025.
37. Murshudov GN, Vagin AA, Dodson EJ. Refinement of macromolecular structures by the maximum-likelihood method. Acta Crystallogr D Biol Crystallogr. 1997; 53:240–255. [PubMed: 15299926]
38. Emsley P, Cowtan K. Coot: model-building tools for molecular graphics. Acta Crystallogr D Biol Crystallogr. 2004; 60:2126–2132. [PubMed: 15572765]
39. Adams PD, Grosse-Kunstleve RW, Hung LW, Ioerger TR, McCoy AJ, Moriarty NW, Read RJ, Sacchettini JC, Sauter NK, Terwilliger TC. PHENIX: building new software for automated crystallographic structure determination. Acta Crystallogr D Biol Crystallogr. 2002; 58:1948–1954. [PubMed: 12393927]
40. Painter J, Merritt EA. Optimal description of a protein structure in terms of multiple groups undergoing TLS motion. Acta Crystallogr D, Biol Crystallogr. 2006; 62:439–450. [PubMed: 16552146]
41. Estevez J, Vilanova E. Model equations for the kinetics of covalent irreversible enzyme inhibition and spontaneous reactivation: esterase and organophosphorus compounds. Crit Rev Toxicol. 2009; 39:427–448. [PubMed: 19514915]
42. Estevez J, Barril J, Vilanova E. Inhibition with spontaneous reactivation and the “ongoing inhibition” effect of esterases by biotinylated organophosphorus compounds: S9B as a model. Chem-Biol Interact. 2010; 187:397–402. [PubMed: 20493177]
43. Estevez J, Garcia-Perez A, Barril J, Vilanova E. Inhibition with spontaneous reactivation of carboxyl esterases by organophosphorus compounds: paraoxon as a model. Chem Res Toxicol. 2011; 24:135–143. [PubMed: 21155548]
44. Masson P, Schopfer LM, Froment MT, Debouzy JC, Nachon F, Gillon E, Lockridge O, Hrabovska A, Goldstein BN. Hysteresis of butyrylcholinesterase in the approach to steady-state kinetics. Chem-Biol Interact. 2005; 157–158:143–152.
45. Shenouda J, Green P, Sultatos L. An evaluation of the inhibition of human butyrylcholinesterase and acetylcholinesterase by the organophosphate chloryrifos oxon. Toxicol Appl Pharmacol. 2009; 241:135–142. [PubMed: 19699221]
46. Loudwig S, Nicolet Y, Masson P, Fontecilla-Camp JC, Bon S, Nachon F, Goeldner M. Photoreversible inhibition of cholinesterases: catalytic serine-labeled caged butyrylcholinesterase. ChemBioChem. 2003; 4:762–767. [PubMed: 12898628]
47. Pietsch M, Christian L, Inhester T, Petzold S, Gutschow M. Kinetics of inhibition of acetylcholinesterase in the presence of acetonitrile. FEBS J. 2009; 276:2292–2307. [PubMed: 19292865]
48. Eto M. Studies on biologically active organophosphorus compounds. J Pestic Sci. 1981; 6:365–375.
49. Eto M, Fukuhara N, Kuwano E, Koyama H. Molecular structure and conformation of 4H-1,3,2-benzodioxaphosphorins, including the insecticide salithion. Agric Biol Chem. 1981; 45:915–923.
50. Eto M. Functions of phosphorus moiety in agrochemical molecules. Biosci Biotech Biochem. 1997; 61:1–11.

51. Worek F, Thiermann H, Szinicz L, Eyer P. Kinetic analysis of interactions between human acetylcholinesterase, structurally different organophosphorus compounds and oximes. Biochem Pharmacol. 2004; 68:2237–2248. [PubMed: 15498514]
52. Toia RF, Casida JE. Phosphorylation, “aging”, and possible alkylation reactions of saligenin cyclic phosphorus esters with α-chymotrypsin. Biochem Pharmacol. 1979; 28:211–216. [PubMed: 426836]
53. Li B, Nachon F, Froment MT, Verdier L, Debouzy JC, Brasme B, Gillon E, Schopfer LM, Lockridge O, Masson P. Binding and hydrolysis of soman by human serum albumin. Chem Res Toxicol. 2008; 21:421–431. [PubMed: 18163544]
54. Li H, Schopfer LM, Nachon F, Froment MT, Masson P, Lockridge O. Aging pathways for organophosphate-inhibited human butyrylcholinesterase. Toxicol Sci. 2007; 100:136–145. [PubMed: 17698511]
55. Shafferman A, Ordentlich A, Barak D, Stein D, Ariel N, Velan B. Aging of phosphylated human acetylcholinesterase: catalytic processes mediated by aromatic and polar residues of the active centre. Biochem J. 1996; 318:833–840. [PubMed: 8836126]
56. Viragh C, Akhmetshin R, Kovach IM, Broomfield C. Unique push-pull mechanism of dealkylation in soman-inhibited cholinesterases. Biochemistry. 1997; 36:8243–8252. [PubMed: 9204869]
57. Sanson B, Nachon F, Colletier JP, Froment MT, Toker L, Greenblatt HM, Sussman JL, Ashani Y, Masson P, Silman I, Weik M. Crystallographic snapshots of nonaged and aged conjugates of soman with acetylcholinesterase, and a ternary complex of the aged conjugate with pralidoxime. J Med Chem. 2009; 52:7593–7603. [PubMed: 19642642]
58. Kovach IM. Stereochemistry and secondary reactions in the irreversible inhibition of serine hydrolases by organophosphorus compounds. J Phys Org Chem. 2004; 17:602–604.
59. Kropp TJ, Richardson RJ. Aging of mipafox-inhibited human acetylcholinesterase proceeds by displacement of both isopropylamine groups to yield a phosphate adduct. Chem Res Toxicol. 2006; 19:334–339. [PubMed: 16485911]
60. Kropp TJ, Richardson RJ. mechanism of aging of mipafox-inhibited butyrylcholinesterase. Chem Res Toxicol. 2007; 20:504–510. [PubMed: 17323978]
61. Worek F, Eyer P, Szinicz L. Inhibition, reactivation and aging kinetics of cyclohexylmethylphosphonofluoridate- inhibited human cholinesterases. Arch Toxicol. 1998; 72:580–587. [PubMed: 9806430]
62. Schopfer LM, Voelker T, Bartels CF, Thompson CM, Lockridge O. Reaction kinetics of biotinylated organophosphorus toxicant, FP-biotin, with human acetylcholinesterase and human butyrylcholinesterase. Chem Res Tox. 2005; 18:747–754.
63. Raveh L, Grunwald J, Marcus D, Papier Y, Cohen E, Ashani Y. Human butyrylcholinesterase as a general prophylactic antidotes for nerve agent toxicity. In vitro and in vivo quantitative characterization. Biochem Pharmacol. 1993; 45:2465–2474. [PubMed: 8328984]
64. Amitai G, Moorad D, Adani R, Doctor BP. Inhibition of acetylcholinesterase and butyrylcholinesterase by chlorpyrifos-oxon. Biochem Pharmacol. 1998; 56:293–299. [PubMed: 9744565]
65. Benkovic, SJ.; Schray, KJ. Chemical basis of biological phosphoryl transfer. In: Boyer, PD., editor. The Enzymes. 3. Vol. VIII. Academic Press; New York: 1973. p. 2010-238.
66. Nachon F, Asojo OA, Borgstahl GEO, Masson P, Lockridge O. Role of water in aging of human butyrycholinesterase inhibited by echothiophate: the crystal stucture suggests two alternative mechanisms of aging. Biochemistry. 2005; 44:1154–1162. [PubMed: 15667209]
67. Nachon F, Carletti E, Worek F, Masson P. Aging mechanism of butyrylcholinesterase inhibited by an N-methyl analogue of tabun: implications of the trigonal-bipyramidal transition state rearrangement for the phosphylation or reactivation of cholinesterases. Chem-Biol Interact. 2010; 187:44–48. [PubMed: 20381476]
68. Whittaker M. Plasma cholinesterase variants and the anaesthetist. Anaesthesia. 1980; 35:174–197. [PubMed: 6992635]
69. Tenberken O, Thiermann H, Worek F, Reiter G. Chromatographic preparation and kinetic analysis of interactions between tabun enantiomers and acetylcholinesterase. Toxicol Lett. 2010; 195:142–146. [PubMed: 20347021]

70. Cavanagh JB. The toxic effect of triortho-cresyl phosphate on the nervous system; an experimental study in hens. J Neurol Neurosurg Psychiat. 1954; 17:163–172. [PubMed: 13192490]
71. Abou-Donia MB. Organophosphorus ester-induced delayed neurotoxicity. Ann Rev Pharmacol Toxicol. 1981; 21:511–548. [PubMed: 7016015]
72. Lotti M, Moretto A. Promotion of organophosphate induced delayed polyneuropathy by certain esterase inhibitors. Chem-Biol Interact. 1999; 119–120:519–524.
73. Kropp TJ, Glynn P, Richardson RJ. The mipafox-inhibited catalytic domain of human neuropathy target esterase ages by reversible proton loss. Biochemistry. 2004; 43:3716–3722. [PubMed: 15035642]
74. Glynn P. A mechanism for organophosphate-induced delayed neuropathy. Toxicol Lett. 2006; 162:94–97. [PubMed: 16309859]
75. Wu, Y-J.; Chang, P-A. Molecular toxicology of neuropathy target esterase. In: Satoh, T.; Gupta, RC., editors. Anticholinesterase Pesticides: Metabolism Neurotoxicity and Epidemiology. John Wiley & Sons; 2010. p. 109-120.
76. Read DJ, Li Y, Chao MV, Cavanagh JB, Glynn P. Organophosphates induce distal axonal damage, but not brain oedema, by inactivating neuropathy target esterase. Toxicol Appl Pharmacol. 2010; 245:108–115. [PubMed: 20188121]
77. Rainier S, Bui M, Mark E, Thomas D, Tokarz D, Ming L, Delaney C, Richardson RJ, Albers JW, Matsunami N, Stevens J, Coon H, Leppert M, Fink JK. Neuropathy target esterase gene mutations cause motor neuron disease. Am J Hum Genet. 2008; 82:780–785. [PubMed: 18313024]
78. Zaja-Milatovic S, Gupta RC, Aschner M, Milatovic D. Protection of DFP-induced oxidative damage and neurodegeneration by antioxidants and NMDA receptor antagonist. Toxicol Appl Pharmacol. 2009; 240:124–131. [PubMed: 19615394]
79. Schopfer LM, Grigoryan H, Li B, Nachon F, Masson P, Lockridge O. Mass spectral characterization of organophosphate-labeled, tyrosine-containing peptides: characteristic mass fragments and a new binding motif for organophosphates. J Chromatog B. 2010; 878:1297–1311.
80. Li B, Ricordel I, Schopfer LM, Baud F, Megarbane B, Nachon F, Masson P, Lockridge O. Detection of adduct on tyrosine 411 of albumin in humans poisoned by dichlorvos. Toxicol Sci. 2010; 116:23–31. [PubMed: 20395308]
81. Lockridge O, Schopfer LM. Review of tyrosine and lysine as new motifs for organophosphate binding to proteins that have no active site serine. Chem Biol Interact. 2010; 187:344–348. [PubMed: 20211158]

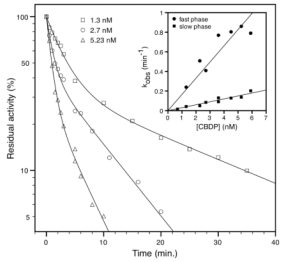

Fig. 1.

Time course of inhibition of hBChE by different concentrations of CBDP in 50 mM sodium phosphate pH 8.0, containing 10% MeOH at 25°C. The solid curve represents the non-linear regression fit using equation (2). Insert: secondary plot used for determination of the bimolecular rate constants of inhibition (k_i and k'_i) for fast and slow phase, according to equation (4).

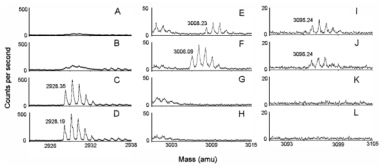

Fig 2.

MALDI TOF mass spectra of the active site tryptic peptide from reactions of BChE with CBDP in the presence and absence of ^{18}O-water.

Reactions of BChE with CBDP were conducted as described in the Materials and Methods section. Masses of interest are shown: 2928 amu $[M+H]^{+1}$ for the unlabeled active site peptide SVTLFGESAGAASVSLHLLSPGSHSLFTR in positive mode; 3006 amu $[M-H]^{-1}$ for the phosphorylated active site peptide in the presence of ^{16}O-water in negative mode; 3008 amu $[M-H]^{-1}$ for the phosphorylated active site peptide in the presence of ^{18}O-water in negative mode; 3096 amu $[M-H]^{-1}$ for the o-cresyl-phosphorylated active site peptide in the presence of ^{18}O-water and ^{16}O-water in negative mode. Limited mass ranges around the masses of interest are shown to emphasize the isotopic splittings and peak resolution, to illustrate the relative intensities of the members of the isotopic families, and to avoid interference from other peptides with greater signal intensities. Panels A, E and I are from the reaction of BChE with CBDP in the presence of ^{18}O-water; panels B, F and J are from the reaction of BChE with CBDP in the presence of ^{16}O-water; panels C, G and K are from an incubation of BChE in ^{18}O-medium without CBDP; and panels D, H and L are from an incubation of BChE in ^{16}O-medium without CBDP. A mass shift of +2 from incorporation of ^{18}O-water is seen only in panel E for the phosphorylated active site peptide of mass 3008, which demonstrates that the P-O bond was broken when the cresylphosphate adduct aged to form phospho-serine. In contrast ^{18}O was not introduced during formation of the cresylphosphate adduct (mass 3096 in panels I and J), which means this adduct resulted from cleavage of the O-C bond.

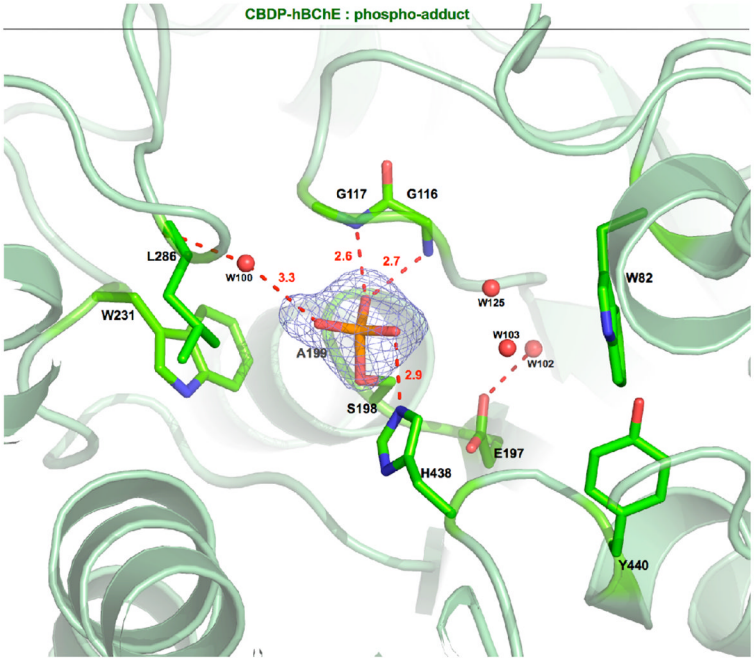

Fig. 3.

Active site view of the phospho-serine-hBChE conjugate. Key residues and the OP adduct are displayed as sticks, with carbon atoms in green, oxygen atoms in red, nitrogen atoms in blue, and the phosphorus atom in orange. Hydrogen bonds are represented as red dashed lines. The Fo − Fc omit map is contoured at 3**σ**.

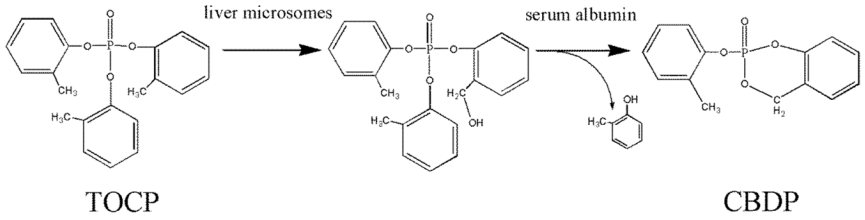

Scheme 1.
Metabolic activation of TOCP to CBDP

$$EH + I \supset \xleftrightarrow{K_I} EH.I \supset \xrightarrow{k_p} EHI$$

Scheme 2.
Reaction of OP**s** with cholinesterases

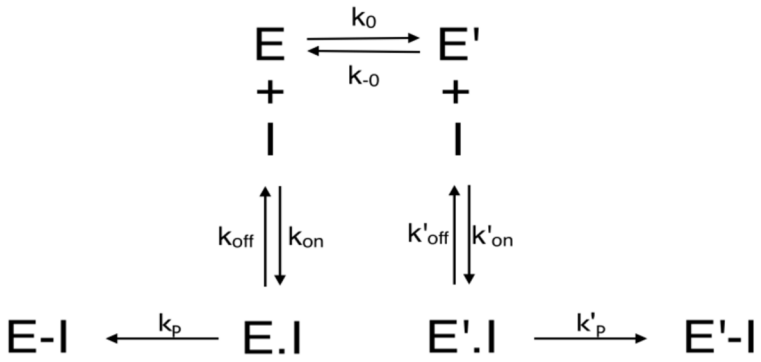

Scheme 3.
Reaction of CBDP with two cholinesterase forms in slow equilibrium

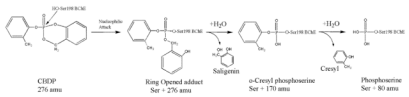

Scheme 4.
Reaction pathway of CBDP with cholinesterases

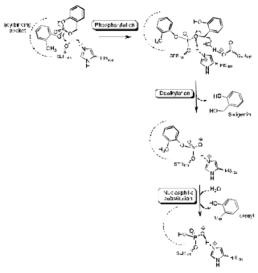

Scheme 5.
Proposed reaction mechanism of CBDP with cholinesterases, leading to phospho serine adduct

Table 1

Bimolecular rate constants (k_i) for inhibition of human AChE and BChE at pH 8.0 and 25°C.

	AChE [a]		BChE	
Enzyme form	**E**	**E′**	**E**	**E′**
k_i ($M^{-1}min^{-1}$) 10% MeOH	$>3.7\times10^6$ [b]	$(1.06\pm0.23)\times10^5$	$(1.5\pm0.2)\times10^8$	$(2.5\pm0.7)\times10^7$
k_i ($M^{-1}min^{-1}$) 5% acetonitrile	ND	$(0.33\pm0.17)\times10^5$	ND	ND
k_i ($M^{-1}min^{-1}$) 0.9% saline	ND	$(0.73\pm0.6)\times10^5$	ND	ND

E, enzyme fast forms; E′ enzyme slow forms

ND, not determined

Experiments were performed in triplicate (mean values ± SE)

[a] experimental k_i values for the E-form of AChE are not listed because the kinetics did not provide a second order rate constant in that instance.

[b] estimated minimum k_i value using $k_p = 0.37\ min^{-1}$ and $K_I \ll 0.1\ \mu M$

Table 2

Data Collection and Refinement Statistics

Data	Phospho-hBChE (pdb code: 2y1k)
space group unit cell parameters, *a*=*b*, *c* (Å)	*I*422 153.77, 127.60
no. of reflections	243 040
no. of unique reflections	25 339
resolution (Å)	40-2.5 (2.6-2.5)
completeness (%)	94.8 (97.4)
*R*merge[a] (%)	8.9 (49.0)
I/ó(I) Redundancy	26.0 (4.8)
Refinement Statistics	6.7 (7.0)
R-factor[b] (*R*-free[c])	18.3 (24.6)
no. of atoms	
protein	4 180
solvent	250
others	154
mean *B*-factor (Å^2)	36.0
RMS from ideality	0.018
bond length (Å)	1.954
angles (deg)	0.151
chiral (Å^3)	

[a] Rmerge = (Σ | I − <I> |)/ΣI, where *I* is the observed intensity and <I> is the average intensity obtained from multiple observations of symmetry related reflections after rejections.

[b] R-factor=Σ |Fo − |Fc||/Σ |Fo|, Fo and Fc are observed and calculated structure factors

[c] R-free set uses 5% of randomly chosen reflections.